Applied Mathematics and Mechanics (English Edition), 2007, **28**(1):119–125

Superconvergence analysis of Wilson element on anisotropic meshes *

SHI Dong-yang (石东洋)[1], LIANG Hui (梁慧)[2]

(1. Department of Mathematics, Zhengzhou University, Zhengzhou 450052, P. R. China;
2. Department of Mathematics, Harin Institute of Technology, Harbin 150001, P. R. China)

(Communicated by ZHONG Wan-xie)

Abstract The Wilson finite element method is considered to solve a class of two-dimensional second order elliptic boundary value problems. By using of the particular structure of the element and some new techniques, we obtain the superclose and global superconvergence on anisotropic meshes. Numerical example is also given to confirm our theoretical analysis.

Key words Anisotropic meshes, Wilson element, superclose, superconvergence

Chinese Library Classification O242.21
2000 Mathematics Subject Classification 65N30, 65N15
Digital Object Identifier(DOI) 10.1007/s 10483-007-0114-1

Introduction

Wilson element has very good numerical results in engineering computation and numerous studies have been devoted to its convergence and superconvergence analysis (see Refs.[1–6]). Especially, Z. C. Shi, B. Jiang and W. M. Xue[2] have studied its superconvergence at vertices, midpoints of sides of the element on a class of so called uniform partition, i.e., all lengths of edges of the element in x-direction are equal and so are all in y-direction. Q. Lin and N. N. Yan[4] have also studied its global superconvergence by using integral identities. However, as far as we know, all of the superconvergence results of Wilson element up to now are dependent of the restriction of classical regularity assumption $h_K/\rho_K \le c$ and the quasi-uniform assumption $h/\tilde{h} \le c$. Here, K is an element, h_K and ρ_K are the diameters of K and the biggest circle contained in K respectively, c is a positive constant independent of $h = \max\limits_K h_K$ and $\tilde{h} = \min\limits_K h_K$ (see Ref.[1]) and the function under considered.

It is well known that the solution of the elliptic boundary value problems may have anisotropic behavior in parts of the domain. That is to say, the solution varies significantly only in certain directions, such as singularly perturbed convection-diffusion-reaction problems where boundary or the interior layers appear. Therefore, in view of both theoretical analysis and practical application, the regularity assumption and quasi-uniform assumption are great drawbacks in the finite element methods. In such cases, an obvious idea to reflect this anisotropy and overcome above fatal deficiency is to use anisotropic meshes in discretization. These are stretched elements where the above aspect ratios can be very large or even unbounded. Although this is converse to the conventional isotropy theory, the use of anisotropic discretization allows to achieve the same accuracy with less degrees of freedom and there have appeared some studies focusing on the study of anisotropic finite element methods recently (see Refs.[6–9]). However, the analysis of the superclose and superconvergence for nonconforming elements on anisotropic meshes has seldom been seen in the previous literatures.

* Received Mar.1, 2005; Revised Sep.18, 2006
Project supported by the National Natural Science Foundation of China (No.10371113)
Corresponding author SHI Dong-yang, Professor, Doctor, E-mail: shi_dy@zzu.edu.cn

The main aim of this paper is to study the superclose and global superconvergence of Wilson's element on anisotropic meshes by employing some novel techniques and using some advantages of Wilson element. Numerical example is also given to verify the validity of our theoretical analysis and the element performance. The results obtained in this paper can be regarded as a generalization to Ref.[4]. Moreover, our analysis will be helpful in developing posterior estimates method and designing some adaptive algorithms of numerical solutions for the second order problems.

Consider the following second order elliptic boundary value problem,

$$\begin{cases} -\triangle u = f, & \text{in } \Omega, \\ u|_\Gamma = 0, & \text{on } \Gamma = \partial\Omega, \end{cases} \tag{1}$$

where $\Omega \subset R^2$ is rectangular domain, $f \in L^2(\Omega)$.

The weak form of Eq.(1) is to find $u \in H_0^1(\Omega) = V$, such that

$$a(u, v) = f(v), \quad \forall\ v \in V, \tag{2}$$

where $a(u,v) = \int_\Omega \nabla u \cdot \nabla v dxdy,\ f(v) = \int_\Omega f v dxdy$.

1 Superclose analysis

For the sake of simplicity, let $\Omega \subset R^2$ be a bounded rectangular domain in $x-y$ plane with the boundary $\partial\Omega$ paralleling to x-axis and y-axis respectively. J_h is a rectangular triangulation of Ω. $\forall K \in J_h$, assume the central point be (x_K, y_K) and four vertices be $d_1 = (x_K - h_{x,K}, y_K - h_{y,K})$, $d_2 = (x_K + h_{x,K}, y_K - h_{y,K})$, $d_3 = (x_K + h_{x,K}, y_K + h_{y,K})$ and $d_4 = (x_K - h_{x,K}, y_K + h_{y,K})$, where $2h_{x,K}$ and $2h_{y,K}$ are the lengths of two edges of K in x-direction and y-direction respectively. Let $h_x = \max\limits_{K\in J_h} h_{x,K}$, $h_y = \max\limits_{K\in J_h} h_{y,K}$, $h_{\max} = \max(h_x, h_y)$. $\hat{K} = [-1,1]\times[-1,1]$ be the reference element in $\xi - \eta$ plane with vertices $\hat{d}_1 = (-1,-1), \hat{d}_2 = (1,-1), \hat{d}_3 = (1,1)$ and $\hat{d}_4 = (-1,1)$. Let V_0^h be Wilson's finite element space[2,4]. Then the approximation problem of Eq.(2) is to find $R_h u \in V_0^h$, such that

$$a_h(R_h u, v_h) = f(v_h), \quad \forall v_h \in V_0^h, \tag{3}$$

where $a_h(u,v) = \sum\limits_K \int_K \nabla u \cdot \nabla v dxdy$.

Let $\bar{V}_h^0 = \{\overline{R_h u} | \overline{R_h u} \in Q_1(K)$ is determined by its function values at four vertices of $K, \overline{R_h u}|_{\partial\Omega} = 0\}$, $\overline{R_h u} \in \bar{V}_0^h$ be the solution satisfies

$$a_h(\overline{R_h u}, v_h) = f(v_h), \quad \forall v_h \in \bar{V}_0^h. \tag{4}$$

It can be verified that

$$a_h(R_h u - \overline{R_h u}, v_h) = a_h(u - \overline{R_h u}, v_h) = 0, \quad \forall v_h \in \bar{V}_0^h. \tag{5}$$

In our forgoing analysis, the following anisotropic inverse inequality plays an essential role.

Lemma 1 $\forall\ v \in V_0^h$ *and* $\forall\ K \in \Gamma_h$, *there hold*

$$\|v_{xx}\|_{0,K} \le c h_x^{-1} \|v_x\|_{0,K}, \quad \|v_{yy}\|_{0,K} \le c h_y^{-1} \|v_y\|_{0,K}. \tag{6}$$

Proof We only prove the first inequality of Ref.(6).

$$\begin{aligned} \|v_{xx}\|_{0,\ K}^2 &= \int_K v_{xx}^2 dxdy = c \int_{\widehat{K}} \hat{v}_{\xi\xi}^2 h_x^{-4} h_x h_y d\xi d\eta = c h_x^{-3} h_y |\hat{v}_{\xi\xi}|_{0,\widehat{K}}^2 \le c h_x^{-3} h_y \|\hat{v}_\xi\|_{1,\widehat{K}}^2 \\ &\le c h_x^{-3} h_y \|\hat{v}_\xi\|_{0,\widehat{K}}^2 = c h_x^{-3} h_y \|v_x\|_{0,K}^2 h_x^2 (h_x h_y)^{-1} = c h_x^{-2} \|v_x\|_{0,K}^2. \end{aligned}$$

Lemma 2 *Suppose $u \in H^3(\Omega) \cap H_0^1(\Omega)$ and $i_h u$ is the bilinear interpolation of u, $w = u - i_h u$, then there hold*

$$\int_\Omega w_x v_x dxdy = ch_y^2 |u|_3 |v|_1, \quad \int_\Omega w_y v_y dxdy = ch_x^2 |u|_3 |v|_1, \quad v \in \bar{V}_0^h. \tag{7}$$

Proof By Lemma 1 and the techniques provided in Ref.[4], we can get the desired results.

Based on Lemma 1 and Lemma 2, we can deduce the following superclose property.

Theorem 3 *Suppose $u \in H^3(\Omega) \cap H_0^1(\Omega)$ and $\overline{R_h u}$ are the solution of Eqs.*(1) *and* (4) *respectively, then*

$$\|\overline{R_h u} - i_h u\|_h \le ch_{\max}^2 |u|_3, \tag{8}$$

where $\|\cdot\|_h^2 = \sum_K |\cdot|_{1,K}^2$.

Proof By Lemma 2 and Eq.(5) we have

$$a(\overline{R_h u} - i_h u, v) = a(u - i_h u, v) + a(\overline{R_h u} - u, v) \le ch_{\max}^2 |u|_3 |v|_1,$$

taking $v = \overline{R_h u} - i_h u$ in above inequality and using the coercive property of $a(\cdot,\cdot)$ yield the desired result.

Lemma 4 *Let $R_h u$ be the solution of Eq.*(3), *under the assumption of Theorem* 3, *we have*

$$i_h R_h u = \overline{R_h u}. \tag{9}$$

Proof Since $\bar{V}_0^h \subset V_0^h$, $\forall v \in \bar{V}_0^h$, noticing that $|R_h u|_{3,K} = 0$ and using of Theorem 3, we have

$$\begin{aligned} a(i_h R_h u - \overline{R_h u}, v) &= a(i_h R_h u - R_h u, v) \\ &= \sum_K \int_K \nabla(i_h R_h u - R_h u) \cdot \nabla v dxdy \\ &= O(h^2) \sum_K |R_h u|_{3,K} \|v\|_{1,K} = 0. \end{aligned} \tag{10}$$

Taking $v = i_h R_h u - \overline{R_h u} \in \bar{V}_0^h$ in Eq.(10) yields the desired result.

By Theorem 3 and Lemma 4, we can get the superclose property of Wilson's element.

Theorem 5 *Under the same assumptions of Theorem* 3, *we have*

$$\|\overline{R_h u} - i_h u\|_h \le ch^2 |u|_3. \tag{11}$$

2 Superconvergence analysis

In order to get the global superconvergence, let J_{2h} be a family of anisotropic meshes. J_h can be obtained by dividing each element of J_{2h} into four equal elements $K_i (i = 1, 2, 3, 4)$. Let $\tilde{K} \in J_{2h}$, $\tilde{K} = \bigcup_{i=1}^{4} K_i$. Then we can construct the post-processing interpolation operator Π_{2h}^2 on $V_0^h \cup H^3(\Omega)$ satisfying

$$\Pi_{2h}^2|_{\tilde{K}} : V_0^h|_{\tilde{K}} \cup H^3(\tilde{K}) \to Q_2(\tilde{K}), \tag{12}$$

$\Pi_{2h}^2 v(a_i) = v(a_i), i = 1, 2, \ldots, 9$. Here $Q_2(\tilde{K})$ denotes the biquadratic polynomial space of x and y on $\tilde{K}$. It is easy to see that

$$\Pi_{2h}^2(i_h w) = \Pi_{2h}^2 w, \quad \forall w \in V_0^h \cup H^3(\Omega). \tag{13}$$

Lemma 6 *For above Π_{2h}^2, there hold*

$$\|u - \Pi_{2h}^2 u\|_{\ell,\Omega} \le c h_{\max}^{1+\gamma-\ell} \|u\|_{\gamma+1,\Omega}, \quad \forall u \in H^3(\Omega), \quad 1 \le \gamma \le 2, \quad \ell = 0, 1, \tag{14}$$

$$\|(\Pi_{2h}^2 v)\|_h \le c\|v\|_h, \quad \forall v \in V_0^h. \tag{15}$$

Proof Estimate (14) can be proved by the same method as in Ref.[3]. Since

$$\begin{aligned}\|(\Pi_{2h}^2 v)_x\|_{0,\tilde{K}}^2 &= \int_{\tilde{K}} (\Pi_{2h}^2 v)_x^2 dxdy = \int_{\widehat{K}} \widehat{(\Pi_{2h}^2 v)}_\xi^2 h_{\tilde{K}_x}^{-2} h_{\tilde{K}_x} h_{\tilde{K}_y} d\xi d\eta = h_{\tilde{K}_x}^{-1} h_{\tilde{K}_y} \|\widehat{(\Pi_{2h}^2 v)}_\xi\|_{0,\widehat{K}}^2 \\ &\le c h_{\tilde{K}_x}^{-1} h_{\tilde{K}_y} \|\hat{v}_\xi\|_{0,\widehat{K}}^2 = c h_{\tilde{K}_x}^{-1} h_{\tilde{K}_y} \int_{\tilde{K}} v_x^2 h_{\tilde{K}_x}^2 h_{\tilde{K}_x}^{-1} h_{\tilde{K}_y}^{-1} dxdy = c\|v_x\|_{0,\tilde{K}}^2,\end{aligned} \tag{16}$$

we have

$$\|(\Pi_{2h}^2 v)_x\|_{0,\tilde{K}} \le c\|v_x\|_{0,\tilde{K}}, \tag{17}$$

similarly

$$\|(\Pi_{2h}^2 v)_y\|_{0,\tilde{K}} \le c\|v_y\|_{0,\tilde{K}}. \tag{18}$$

By summing Eqs.(17) and (18) over all elements of J_h, we can get Eq.(15). The proof is completed.

Theorem 7 *Under the hypothesis of Theorem* 3, *there holds the following superconvergence estimate on anisotropic meshes*

$$\|u - \Pi_{2h}^2 i_h R_h u\|_h \le c h_{\max}^2 |u|_3.$$

Proof By Lemma 4 and Theorem 5, we have

$$\begin{aligned}\|\Pi_{2h}^2 i_h R_h u - u\|_h &\le \|u - \Pi_{2h}^2 (i_h u)\|_h + \|\Pi_{2h}^2 i_h R_h u - \Pi_{2h}^2 (i_h u)\|_h \\ &\le \|u - \Pi_{2h}^2 u\|_h + \|\Pi_{2h}^2 (i_h u - i_h R_h u)\|_h \\ &\le c(h_{\max}^2 |u|_3 + \|i_h u - i_h R_h u\|_h) \\ &\le c h_{\max}^2 |u|_3.\end{aligned}$$

3 Numerical example

In order to verify our theoretical analysis and examine the performance of the Wilson element on anisotropic meshes, we consider problem (1) with $\Omega = [0,1]^2 \subset R^2$ and

$$\begin{aligned}f = -\triangle u = &-2(1 - \mathrm{e}^{-\frac{x}{\varepsilon}})(1-x) - \frac{2\mathrm{e}^{-\frac{y}{\varepsilon}}(1-x)x}{\varepsilon} + 2(-1 + \mathrm{e}^{-\frac{y}{\varepsilon}})(1-y) \\ &- \frac{\mathrm{e}^{-\frac{y}{\varepsilon}}(1-x)x(1-y)}{\varepsilon} + \left(-\frac{2\mathrm{e}^{-\frac{x}{\varepsilon}}}{\varepsilon} - \frac{\mathrm{e}^{-\frac{x}{\varepsilon}}(1-x)}{\varepsilon^2}\right) y(1-y),\end{aligned}$$

we can verify that

$$u = (1-x)y(1-y)(1 - \mathrm{e}^{-x/\varepsilon}) + (1-y)x(1-x)(1 - \mathrm{e}^{-y/\varepsilon})$$

is a solution of Eq.(1).

Because $u(x, y)$ varies intensively near two edges of Ω ($x = 0$ and $y = 0$) when ε is small enough, we divide Ω with different meshes in different parts. We first determine the boundary layer, which is denoted by a. Then we divide each edges of Ω into two parts according to a, and

denote the boundary layer of the two edges of Ω ($x=0$ and $y=0$) by $\Omega_1=(0,a)\times(0,1)$ and $\Omega_2=(0,1)\times(0,a)$ respectively. In this way, Ω is composed of four parts: $\Omega_1\cap\Omega_2$, $\Omega-\Omega_1\cup\Omega_2$, $\Omega_1-\Omega_1\cap\Omega_2$ and $\Omega_2-\Omega_1\cap\Omega_2$.

Let p be the ratio of the boundary layer's subdividing cost to the whole subdividing cost along one edge. For example, if we divide one edge into n small parts, then the boundary layer takes $n\cdot p$ equal small parts, and the remain part of this edge takes $n\cdot(1-p)$ equal small parts. We can get different meshes when p varies. Here we take $p=1/2$ and $p=3/5$ to get two kinds of meshes (see Fig.1, Mesh 1 and Mesh 2).

We consider two cases: $\varepsilon=0.05$ and $\varepsilon=0.02$. The graphs of solution $u(x,y)$ are listed in Fig.2 and Fig.3 respectively. In following tables 1–8, α represents the average convergence order, m and n denote the number of subdividing element along x-direction and y-direction respectively.

In Table 9, let $h_{\rm L}$ and $h_{\rm S}$ denote the lengths of the longer edge and the shorter one of K respectively.

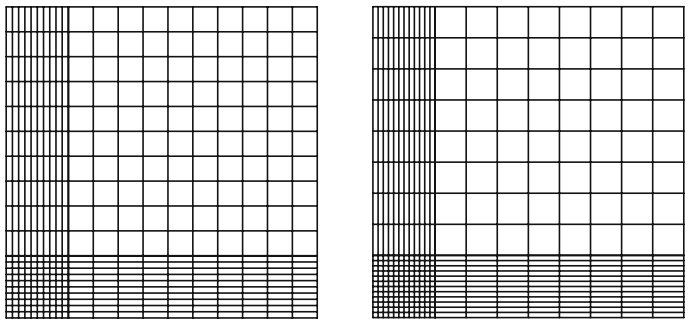

Fig.1 Two kinds of meshes

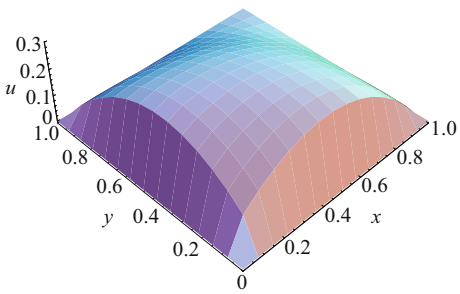

Fig.2 $u(x,y)$ ($\varepsilon=0.05$)

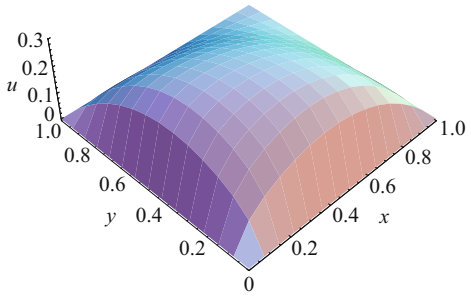

Fig.3 $u(x,y)$ ($\varepsilon=0.02$)

Table 1 Approximation results with $\varepsilon=0.05, a=0.18$ and $p=1/2$

$m\times n$	$\|u-R_hu\|_0$	$\|u-R_hu\|_h$	$\|\overline{R_hu}-i_hu\|_h$	$\|u-\Pi^2_{2h}i_hR_hu\|_h$
40×40	2.7514797×10^{-3}	2.077063469×10^{-1}	1.0974888×10^{-3}	4.8760150×10^{-3}
80×80	6.886549×10^{-4}	1.039749585×10^{-1}	2.749891×10^{-4}	1.2474177×10^{-3}
160×160	1.722130×10^{-4}	5.20027540×10^{-2}	6.87865×10^{-5}	3.140017×10^{-4}
α	1.99897	0.998943	1.99797	1.97848

Table 2 Approximation results with $\varepsilon = 0.05, a = 0.18$ and $p = 3/5$

$m \times n$	$\|u - R_h u\|_0$	$\|u - R_h u\|_h$	$\|\overline{R_h u} - i_h u\|_h$	$\|u - \Pi_{2h}^2 i_h R_h u\|_h$
40×40	4.2956967×10^{-3}	$2.595329278 \times 10^{-1}$	1.6669605×10^{-3}	4.3491402×10^{-3}
80×80	1.0749326×10^{-3}	$1.298887720 \times 10^{-1}$	4.177859×10^{-4}	1.1667889×10^{-3}
160×160	2.687965×10^{-4}	$6.49597409 \times 10^{-2}$	1.045139×10^{-4}	2.985274×10^{-4}
α	1.99915	0.99915	1.99773	1.9328

Table 3 Approximation results with $\varepsilon = 0.05, a = 0.20$ and $p = 1/2$

$m \times n$	$\|u - R_h u\|_0$	$\|u - R_h u\|_h$	$\|\overline{R_h u} - i_h u\|_h$	$\|u - \Pi_{2h}^2 i_h R_h u\|_h$
40×40	2.5961414×10^{-3}	$2.011467162 \times 10^{-1}$	1.0287218×10^{-3}	5.6307887×10^{-3}
80×80	6.499124×10^{-4}	$1.007135721 \times 10^{-1}$	2.577927×10^{-4}	1.4254743×10^{-3}
160×160	1.625331×10^{-4}	$5.03743762 \times 10^{-2}$	6.44870×10^{-5}	3.576058×10^{-4}
α	1.99878	0.998743	1.99785	1.98846

Table 4 Approximation results with $\varepsilon = 0.05, a = 0.20$ and $p = 3/5$

$m \times n$	$\|u - R_h u\|_0$	$\|u - R_h u\|_h$	$\|\overline{R_h u} - i_h u\|_h$	$\|u - \Pi_{2h}^2 i_h R_h u\|_h$
40×40	4.0520037×10^{-3}	$2.512377089 \times 10^{-1}$	1.5479066×10^{-3}	4.3986615×10^{-3}
80×80	1.0140848×10^{-3}	$1.257552398 \times 10^{-1}$	3.879344×10^{-4}	1.1337281×10^{-3}
160×160	2.535892×10^{-4}	$6.28947300 \times 10^{-2}$	9.70451×10^{-5}	2.863042×10^{-4}
α	1.99904	0.999021	1.99776	1.9708

Table 5 Approximation results with $\varepsilon = 0.02, a = 0.05$ and $p = 1/2$

$m \times n$	$\|u - R_h u\|_0$	$\|u - R_h u\|_h$	$\|\overline{R_h u} - i_h u\|_h$	$\|u - \Pi_{2h}^2 i_h R_h u\|_h$
40×40	$1.37779677 \times 10^{-2}$	$9.131560630 \times 10^{-1}$	2.8023323×10^{-3}	$3.99815970 \times 10^{-2}$
80×80	3.4493909×10^{-3}	$4.571854644 \times 10^{-1}$	7.085860×10^{-4}	$1.66707959 \times 10^{-2}$
160×160	8.627183×10^{-4}	$2.286826074 \times 10^{-1}$	1.777241×10^{-4}	5.1238532×10^{-3}
α	1.99867	0.998758	1.98947	1.49873

Table 6 Approximation results with $\varepsilon = 0.02, a = 0.07$ and $p = 1/2$

$m \times n$	$\|u - R_h u\|_0$	$\|u - R_h u\|_h$	$\|\overline{R_h u} - i_h u\|_h$	$\|u - \Pi_{2h}^2 i_h R_h u\|_h$
40×40	$1.31839998 \times 10^{-2}$	$8.931047108 \times 10^{-1}$	2.4506205×10^{-3}	$1.55100272 \times 10^{-2}$
80×80	3.3004158×10^{-3}	$4.471448302 \times 10^{-1}$	6.161844×10^{-4}	6.0387176×10^{-3}
160×160	8.253884×10^{-4}	$2.236483305 \times 10^{-1}$	1.542925×10^{-4}	1.8218848×10^{-3}
α	1.99879	0.998799	1.99471	1.55655

Table 7 Approximation results with $\varepsilon = 0.02, a = 0.18$ and $p = 3/5$

$m \times n$	$\|u - R_h u\|_0$	$\|u - R_h u\|_h$	$\|\overline{R_h u} - i_h u\|_h$	$\|u - \Pi_{2h}^2 i_h R_h u\|_h$
40×40	$1.56001908 \times 10^{-2}$	$9.598546147 \times 10^{-1}$	2.6542626×10^{-3}	$2.75604182 \times 10^{-2}$
80×80	3.9182545×10^{-3}	$4.821773487 \times 10^{-1}$	6.68087×10^{-4}	7.0725399×10^{-3}
160×160	9.807140×10^{-4}	$2.413729924 \times 10^{-1}$	1.673196×10^{-4}	1.7800004×10^{-3}
α	1.9958	0.995778	1.99382	1.97639

Table 8 Approximation results with $\varepsilon = 0.02, a = 0.20$ and $p = 3/5$

$m \times n$	$\|u - R_h u\|_0$	$\|u - R_h u\|_h$	$\|\overline{R_h u} - i_h u\|_h$	$\|u - \Pi_{2h}^2 i_h R_h u\|_h$
40×40	$1.47167111 \times 10^{-2}$	$9.284784397 \times 10^{-1}$	2.5023655×10^{-3}	$3.36911149 \times 10^{-2}$
80×80	3.7000743×10^{-3}	$4.668842181 \times 10^{-1}$	6.305381×10^{-4}	8.6972803×10^{-3}
160×160	9.263422×10^{-4}	$2.337771517 \times 10^{-1}$	1.579589×10^{-4}	2.1923313×10^{-3}
α	1.99489	0.99487	1.99284	1.97102

It can be seen from above tables that the numerical results rely on the choices of a and p which ensure that the subdivisions are consistent with the physical characters of real solution $u(x, y)$. Meanwhile, on anisotropic meshes, when $h \longrightarrow 0$, $\|u - \Pi_{2h}^2 i_h R_h u\|_h$, $\|u - R_h u\|_h$ and $\|\overline{R_h u} - i_h u\|_h$ converge at rates of $O(h^2)$, $O(h)$ and $O(h^2)$ respectively, which coincide with our theoretical analysis.

Table 9 Values of $\max(h_{\mathrm{L}}/h_{\mathrm{S}})$

	$p = 1/2$	$p = 3/5$
$a = 0.18$	4.555556	6.833333
$a = 0.20$	4.000000	6.00000
$a = 0.05$	19.00000	24.00000
$a = 0.07$	13.285704	17.14286

References

[1] Ciarlet P G. The finite element method for elliptic problem[M]. Amsterdam: North-Holland, 1978.

[2] Shi Z C, Jiang B, Xue W M. A new superconvergence property of Wilson nonconforming finite element[J]. *Numer Math*, 1997, **78**:259–268.

[3] Luo Ping, Lin Qun. High accuracy analysis of the Wilson element[J]. *J of Comput Math*, 1999, **17**(2):113–124.

[4] Lin Qun, Yan Ningning. The construction and analysis of high accurate finite element methods[M]. Shijiazhuang: Hebei University Press, 1996 (in Chinese).

[5] Shi Dongyang, Chen Shaochun. A kind of improved Wilson arbitrary quadrilateral elements[J]. *J Numer Math, J Chinese University*, 1994, **16**(2):161–167 (in Chinese).

[6] Chen Shaochun, Zhao Yongcheng, Shi Dongyang. Anisotropic interpolation with application to nonconforming elements[J]. *Appl Numer Math*, 2004, **49**:135–152.

[7] Zienissek A, Vanmaele M. The interpolation theorem for narrow quadrilateral isotropic metric finite elements[J]. *Numer Math*, 1995, **72**:123–141.

[8] Apel Th, Dobrowolski M. Anisotropic interpolation with applications to the finite element method[J]. *Computing*, 1992, **47**:277–293.

[9] Apel Th. Anisotropic finite elements: local estimate and applications[M]. Stuttgart, Leipzig: B.G.Teubner, 1999.